

A High Thermal Dissipation Performance Polyethyleneterephthalate Heat Pipe

Chih-Chieh Chen, Chih-Hao Chen, Guan-Wei Wu, Sih-Li Chen

Abstract—A high thermal dissipation performance polyethylene terephthalate heat pipe has been fabricated and tested in this research. Polyethylene terephthalate (PET) is used as the container material instead of copper. Copper mesh and methanol are sealed in the middle of two PET films as the wick structure and working fluid. Although the thermal conductivity of PET (0.15-0.24 W/m·K) is much smaller than copper (401 W/m·K), the experiment results reveal that the PET heat pipe can reach a minimum thermal resistance of 0.146 (°C/W) and maximum effective thermal conductivity of 18,310 (W/m·K) with 36.9 vol% at 26 W input power. However, when the input power is larger than 30 W, the laminated PET will debond due to the high vapor pressure of methanol.

Keywords—PET, heat pipe, thermal resistance, effective thermal conductivity.

I. INTRODUCTION

IN recent years, heat pipe have replaced heat sinks for high heat dissipation applications because of its higher efficiency of heat removal. As the processing speed of central processing unit (CPU) progress from MHz to GHz, single-phase air cooling system can no longer meet the heat dissipation demand [1]-[3].

In addition to applications in CPU cooling, heat pipes can also be used in solar energy [4], [5], thermoelectric generator [6], [7] and drying system [8], [9] applications.

A heat pipe is a closed two-phase thermal cycle heat exchanger to transfer large amounts of heat energy with minimal temperature gradient [10]. Heat pipes are mainly composed of three components: a hermetic container, a wick structure and working fluid. The wick structure and working fluid are sealed inside the hermetic container under vacuum.

When the working fluid absorbs heat from a heat source, it evaporates and the vapor traverses to the cooling end. The vapor then releases latent heat and condenses back to liquid state. The wick structures supply capillary pressure for facilitating the return of the liquid to the heat source.

In conventional heat pipes, the container is made of metals. The type of metal to use is based on its compatibility with the working fluid. Incompatibility will induce two problems: etching of the container and inability to fully condense the gas back to liquid state. If the working fluid etches the container

and the container material is dissolved the wick structure will be blocked and may generate hot spots. If the gas is not condensed completely, it will accumulate in the condenser section and the heat transfer efficiency will be reduced. Most heat pipes are made of aluminum (Al), stainless steel (SS) or copper (Cu) [11]-[14]. The steps traditionally involved in manufacturing heat pipes include pipe manufacturing, wick structure fabrication, evacuating, charging, vacuum evacuation and leakage testing. These steps are both time-consuming and relatively expensive.

Recently, many researchers have adopted polymers as the container material for heat pipes. Wang and Peterson developed a flexible micro heat pipe with an array of rectangular or trapezoidal microchannels in a Polypropylene (PP) polymer by extrusion processes [15]. Tanaka et al. demonstrated an ultra-lightweight polyimide-based wickless heat pipe with flexible, inflatable, and deployable functions [16]. Wits et al. integrated the laminated structure of a print circuit board (PCB) to fabricate a flat miniature heat pipe. The microgrooves are realized by a selective plating process, also used for metallic patterning [17]. Oshman et al. applied liquid crystal polymer (LCP) films with copper-filled thermal vias as the case material of micro heat pipe. The wicking structure was a hybrid of copper micropillar and woven mesh [18]. The aforementioned polymer-based heat pipes achieved a reduction in fabrication cost and time, but the heat transfer performance is far from ideal. This is because the thermal conductivity of polymer is much lower than that of metal, therefore heat transfer from the heat source to the working fluid through this polymer interlayer is not very efficient. In this research, we propose a novel approach to fabricate polyethylene terephthalate (PET) heat pipes. PET is a popular substrate material because of its excellent properties such as flexibility, mechanical strength, light transmission, insulating, and chemical resistance [19], [20], to name a few. Furthermore, PET is a thermoplastic polymer which can be easily bonded to itself by lamination. These properties make PET ideal as the container material in place of metals.

C. C. Chen, C. H. Chen, and G. W. Wu are with the Department of Mechanical Engineering, National Taiwan University, Taipei 10617 (e-mail: d98522019@ntu.edu.tw, d00522003@ntu.edu.tw, d6522025@ntu.edu.tw, respectively).

S. L. Chen is with the Department of Mechanical Engineering, National Taiwan University, Taipei 10617 (phone: 886-23366-4497; fax: 886-2363-1808; e-mail: slchen01@ntu.edu.tw).

TABLE I
NOMENCLATURE

Symbol	Quantity	Unit
A	area	m^2
K	thermal conductivity	$\text{W/m}\cdot^\circ\text{C}$
L	length	m
Q	input power	W
R	thermal resistance	$^\circ\text{C/W}$
T	temperature	K
Subscripts		
a	Adiabatic	
c	Condenser	
e	Evaporator	
eff	Effective	

II. THE STRUCTURE AND DIMENSION OF PET HEAT PIPE

A PET heat pipe is constructed composing of four components: PET container, copper tape, copper mesh and rubber support, as shown in Fig. 1. The width, length and thickness of the heat pipe are 20 (mm), 120 (mm) and 1.7 (mm), respectively. The container is made of PET and the wick structure is comprised of a copper mesh with a wire diameter of 100 (μm), spaced 150 (μm) between each other. Rubber is used as a supporting structure to prevent the heat pipe from collapsing under vacuum and to provide space for vapor flow. Copper tape is used to increase the thermal conduction area.

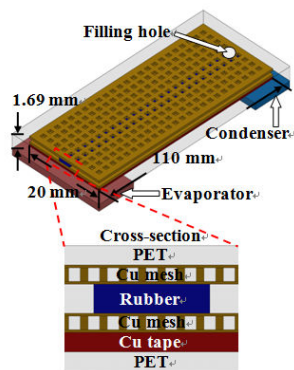


Fig. 1 Schematic of PET heat pipe

III. FABRICATION PROCESS

A. Heat Pipe Container and Wick Structure Fabrication

The fabrication process of PET heat pipe is illustrated in Fig. 2. First a thin film of PET is used and two windows are cut out and attached to a copper tape (Figs. 2 (a), (b)). The function of these two windows is to let the copper tape come in contact with the heat source and heat sink directly, thus circumventing the issue of poor heat conductivity that plagues polymer heat pipes. Then the copper mesh, rubber and another copper mesh are stacked layer-by-layer (Fig. 2 (c)-(e)). Finally a second PET film is covered on top and the entire structure is laminated at 110 ($^\circ\text{C}$) to bond the top and bottom PET layers (Fig. 2 (f)).

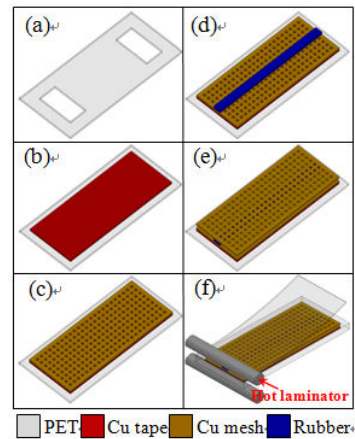


Fig. 2 Fabrication process of PET heat pipe

B. Filling Working Fluid and Vacuum Evacuation

Usually for heat pipes, a vacuum pump is used to remove all gas (air) from the pipe, and then the container is filled partially with working fluid. In PET heat pipes, it is difficult to insert a tube for pumping the air out. For this reason, a vapor pumping method is adopted in this experiment. The vapor pumping method involves first filling the heat pipe with methanol and then immersing it in a hot water bath. When the methanol evaporates, the air will be carried out by the methanol vapor (Fig. 3).

The filling ratio is defined as the volume of working fluid divided by volume of the heat pipe. The volume of the working fluid and the heat pipe is calculated through following three steps: 1. The weight of the heat pipe (including wick structure but without working fluid) is measured. 2. The heat pipe is filled with methanol, and the weight measured. The weight difference (before and after filling with methanol) multiplied by the density of methanol is the total pipe volume. 3. The heat pipe is evacuated using the vapor pumping method and the weight measured. The weight difference (before and after vapor pumping) multiplied by the methanol density is the working fluid volume. Once the desired filling ratio is achieved, the filling hole is sealed with an adhesive tape.

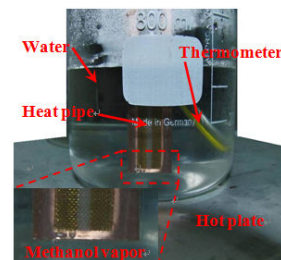


Fig. 3 Vapor pumping method

IV. EXPERIMENTAL SETUP AND PROCEDURES

The experimental setup is shown in Fig. 4. The heat pipe is placed on an X-Y table. A power supply provides power to Polyimide (Pi) film heater for heating the heat pipe. The Pi film heater heated the evaporator and while the condenser is cooled

by convection with 25 ($^{\circ}\text{C}$) ambient temperature. Infrared (IR) thermal camera is used to monitor the temperature distribution of along the heat pipe and real-time thermal images are displayed on a PC screen. The temperature measurement range and maximum resolution of the IR camera are $-40(^{\circ}\text{C})$ - $500(^{\circ}\text{C})$ and $18.5(\mu\text{m}) \times 18.5(\mu\text{m})$ per pixel size (with microscope objective), respectively. The detailed experimental procedures are illustrated in Fig. 5.

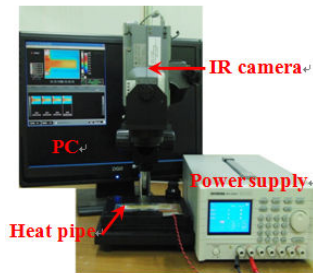


Fig. 4 Experimental setup

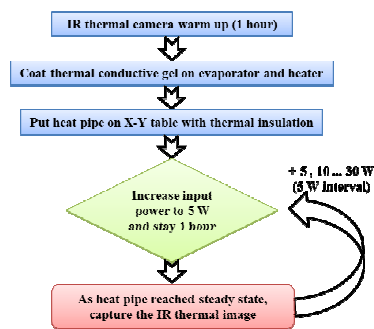


Fig. 5 Experimental procedures

V. EXPERIMENT RESULTS AND DISCUSSION

A. Temperature Observation at Different Filling Ratio

The thermal images of a heat pipe with a 36.9% filling ratio at different input powers are shown in Fig. 6. At 5 (W) and 10 (W), the temperature distribution is stable and the methanol remained in liquid phase. As the input power is increased from 16 (W) to 30 (W), nucleate boiling occurred inside the heat pipe, which results in fast heat transfer from the evaporator to the condenser, as well as an increase in temperature of both the evaporator and the condenser. When the input power is increased to 35 (W), the heat pipe debonded due to high methanol pressure and methanol leaked out from the debonding site.

As depicted in Fig. 7, the two black rectangular areas are the average temperature of evaporator and condenser across all pixels. The red and green rectangular areas are the entire heat pipe and section average temperature. The red and black numbers are the highest and lowest temperature values of a single pixel in each rectangular area, respectively.

The section average temperature along the heat pipe is shown in Fig. 8. When the input power is below 10 (W), little heat is absorbed by the working fluid and the heating

temperature is below its boiling point. Therefore, the methanol remains in liquid phase and the temperature distribution is stable at each section. As input power is increased, methanol continues to absorb heat until the boiling point is reached. The methanol then starts to boil and methanol vapor flows to the condenser rapidly. A great increase in temperature throughout the heat pipe is observed at this stage. At an input power of 30W, more methanol evaporates and very little methanol condenses and flows back to the evaporator. As a result, dry-out occurs and the temperature at the evaporator sharply rises but the temperature of condenser does not. This is because the convection at the condenser cannot remove latent heat any faster.

The section average temperature along the heat pipe for different filling ratios is shown in Fig. 9. At a filling ratio of 18.6%, methanol vapor has lower flow resistance and higher drive pressure, thus only a little liquid methanol participates in heat exchange at evaporator and the heat delivered to the condenser is limited. At a filling ratio of 66.4%, more heat could be taken to the condenser but the flow resistance is higher and the drive pressure is lower [21]. Therefore, both high and low filling ratios result in a relatively large temperature gradient between the evaporator and the condenser. At 36.9 % filling ratio and 26 (W) input power, the average temperature in the evaporator and condenser are 58.94 ($^{\circ}\text{C}$) and 54.86 ($^{\circ}\text{C}$), respectively.

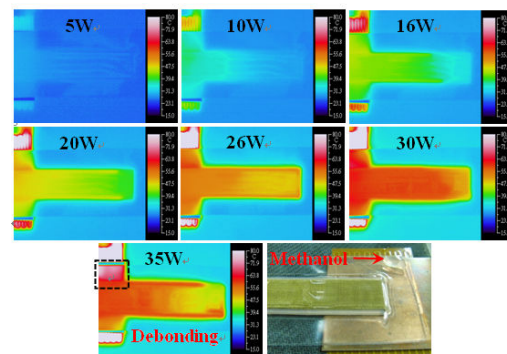


Fig. 6 IR thermal images at 36.9% filling ratio and different input power

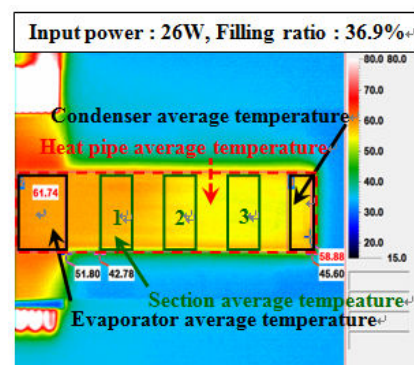


Fig. 7 IR thermal image for calculation the heat pipe average temperature

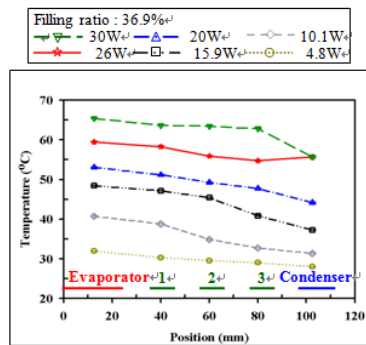


Fig. 8 The position and temperature profile with 36.9% filling ratio

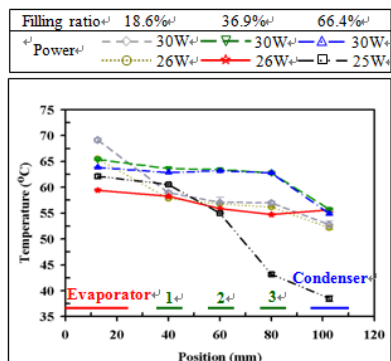


Fig. 9 The position and temperature profile with different filling ratio

B. Influence of Filling Ratio on the Thermal Resistance

The correlation between input power and thermal resistance with different filling ratio is shown in Fig. 10. The thermal resistance (R_{th}) is calculated by

$$R_{th} = \frac{(T_e - T_c)}{Q} \quad (1)$$

where T_e and T_c are the average temperature of evaporator and condenser, respectively, and Q is the input power.

There are three experimental phenomena which can be observed in the PET heat pipe from experiment results. When the heat pipe is subjected to a small heat load (below 10 (W)), the thermal resistance is much higher, which indicates that of the heat pipe is not transferring heat efficiently. This is due to the viscous limit (vapor pressure) of the heat pipe which usually appears at start-up operating stage. This effect is more pronounced at a high filling ratio (66.4%). In this stage the working fluid is in the liquid phase and moves by convection. Therefore, only a minimal heat input is necessary to overcome the viscosity of liquid to produce vapor flow. As the input power is increased, the thermal resistance of the heat pipe drops significantly for a filling ratio of 36.9% as compared to 18.6%. Because the temperature of the working fluid is higher than its boiling point, two-phase flow heat transfer occurs inside the heat pipe and the thermal resistance is reduced with increasing input power (Fig. 11). In this stage, vapor is rapidly delivered to the condenser because of a higher vapor pressure at the evaporator. As a result, the temperature distribution across the

entire heat pipe is more uniform, which also can be observed from IR thermal images. The minimum temperature difference between the evaporator and the condenser is 4.08(°C) at 36.9% filling ratio and 26 (W) input power. Therefore, the minimum thermal resistance of PET heat pipe is 0.146(°C/W). Although a higher vapor pressure reduces thermal resistance, an overly high vapor pressure can burst the heat pipe. In this experiment, the PET films debonded because of the high methanol vapor pressure at 35 W input power (Fig. 12).

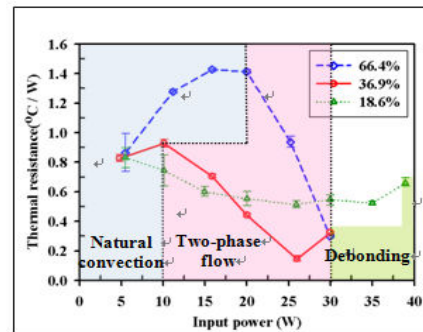


Fig. 10 Thermal resistance variation with different input power

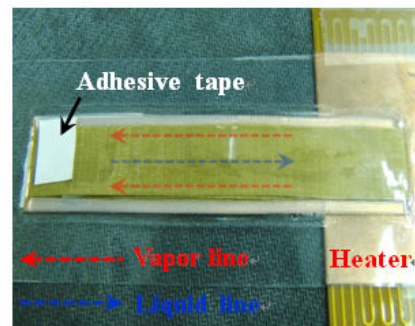


Fig. 11 Two-phase flow in PET heat pipe

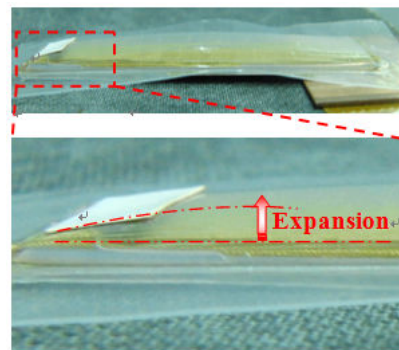


Fig. 12 PET heat pipe debonding

C. Effective Thermal Conductivity of PET Heat Pipe

A heat pipe is essentially a passive two-phase heat transfer device with an extremely high effective thermal conductivity (K_{eff}), much higher than that of a solid body. If the heat pipe works normally, the heat transfer capability can be several hundred to one thousand times that of a piece of copper. The

effective thermal conductivity is expressed by the following equation from 1-D Fourier's law of heat conduction [22], [23].

$$K_{\text{eff}} = \frac{Q}{A} \times \frac{L_{\text{eff}}}{T_e - T_c} \quad (2)$$

where L_{eff} is the effective length which can be calculated as $L_a + (L_e + L_c)/2$, where L_a , L_e , and L_c are the length of the adiabatic, evaporator, and the condenser section, respectively. A is cross-sectional area of heat pipe.

The correlation between input power and effective thermal conductivity with different filling ratios are shown in Fig. 13. The cross-sectional area and length of PET heat pipe are $3.378 \times 10^{-5} (\text{m}^2)$ and $0.09 (\text{m})$, respectively. The minimum temperature difference is $4.34 (^{\circ}\text{C})$ at $26 (\text{W})$ and 36.9% . Therefore, the maximum effective thermal conductivity is $18,310 (\text{W/m}\cdot\text{K})$. This indicates that the effective thermal conductivity of PET heat pipe is about 45 times larger than that of copper.

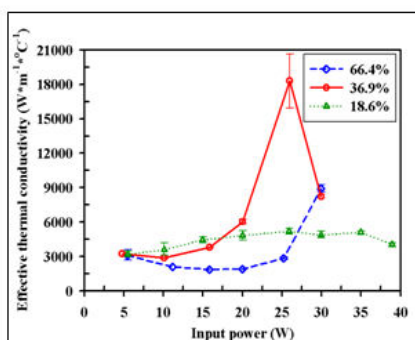


Fig. 13 Effective thermal conductivity

VI. CONCLUSIONS

A high thermal dissipation performance PET heat pipe has been fabricated successfully in this research. Different from previous research which focused on heat pipes with metal or silicon container, we used PET as the container material for heat pipe fabrication. A hot laminator is used to bond two pieces of PET films together to form the heat pipe. This hot lamination method can reduce fabrication cost and time for manufacturing heat pipe. Although the thermal conductivity of PET is much smaller than that of metal, the PET heat pipe still achieved low thermal resistance ($0.146 (^{\circ}\text{C}/\text{W})$) and high effective thermal conductivity ($18,310 (\text{W/m}\cdot\text{K})$) at 36.9% filling ratio and $26 (\text{W})$ input power. The PET heat pipe has the risk of debonding when the input power was increased beyond $30 (\text{W})$. Compared with a copper pipe, PET is an inexpensive, light-weight and easy to seal material. In the future, this high thermal dissipation performance heat pipe may be a reliable and suitable solution for cooling IC with heat generation below than 30 W .

REFERENCE

[1] X. L. Xie, Y. L. He, W. Q. Tao, H. W. Yang, "An experimental investigation on a novel high-performance integrated heat pipe-heat sink

for high-flux chip cooling," *Appl. Therm. Eng.*, vol. 28, pp.433–439, Apr. 2008.

[2] Y. C. Weng, H. P. Cho, C. C. Chang, S. L. Chen, "Heat pipe with PCM for electronic cooling," *Appl. Energy*, vol. 88, pp. 1825–1833, May 2011.

[3] T. Dobre, O. C. Părvulescu, A. Stoica, G. Iavorschi, "Characterization of cooling systems based on heat pipe principle to control operation temperature of high-tech electronic components," *Appl. Therm. Eng.*, vol. 30, pp. 2435–2441, Nov. 2010.

[4] G. Pei, H. Fu, H. Zhu, J. Ji, "Performance study and parametric analysis of a novel heat pipe PV/T system," *Energy*, vol. 37, pp. 384–395, Jan. 2012.

[5] G. Pei, H. Fu, J. Ji, T. Chow, T. Zhang, "Annual analysis of heat pipe PV/T systems for domestic hot water and electricity production," *Energy Conv. Manag.*, vol. 56, pp. 8–21, Apr. 2012.

[6] W. Hea, Y. Su, S. B. Riffat, J. X. Hou, J. Ji, "Parametrical analysis of the design and performance of a solar heat pipe thermoelectric generator unit," *Appl. Energy*, vol. 88, pp. 5083–508, Dec. 2011.

[7] N. Miljkovic, E. N. Wang, "Modeling and optimization of hybrid solar thermoelectric systems with thermosyphons," *Sol. Energy*, vol. 85, pp. 2843–2855, Nov. 2011.

[8] P. Meena, S. Rittidech, N. Poonsa-ad, "Closed-loop oscillating heat-pipe with check valves (CLOHP/CVs) air-preheater for reducing relative humidity in drying systems," *Appl. Energy*, vol. 84, pp. 363–373, Apr. 2007.

[9] S. Rittidech, N. Pipatpaiboon, P. Terdtoon, "Heat-transfer characteristics of a closed-loop oscillating heat-pipe with check valves," *Appl. Energy*, vol. 84, pp.565–577, May 2007.

[10] D. A. Reay, P. A. Kew, *Heat pipes*, 5th ed., Butterworth-Heinemann, Boston, 2006.

[11] K. Take, R. L. Webb, "Thermal performance of integrated plate heat pipe with a heat spreader," *J. Electron. Packag.*, vol. 123, pp. 189–195, Apr. 2000.

[12] S. Lips, F. Lefèvre, J. Bonjour, "Nucleate boiling in a flat grooved heat pipe," *Int. J. Therm. Sci.*, vol. 48, pp. 1273–1278, July 2009.

[13] G. S. Hwang, Y. Nam, E. Fleming, P. Dussinger, Y. S. Ju, M. Kaviani, "Multi-artery heat pipe spreader: Experiment," *Int. J. Heat Mass Transf.*, vol. 53, pp. 2662–2669, June 2010.

[14] J. Wang, "Experimental investigation of the transient thermal performance of a bent heat pipe with grooved surface," *Appl. Energy*, vol. 86, pp. 2030–2037, Oct. 2009.

[15] Y. X. Wang, G. P. Peterson, "Capillary evaporation in microchanneled polymer films," *J. Thermophys. Heat Transf.* vol.17, pp.354–359, July-Sep. 2003.

[16] K. Tanaka, Y. Abe, M. Nakagawa, C. Piccolo, R. Savinoo, "Low-gravity experiments of lightweight flexible heat pipe panels with self-rewetting fluids," *Ann. NY. Acad. Sci.*, vol. 1161, pp. 554–561, Apr. 2009.

[17] W. W. Wits, T. H. J. Vaneker, "Integrated design and manufacturing of flat miniature heat pipes using printed circuit board technology," *IEEE Trans. Compon. Pack. Technol.*, vol. 33, pp. 398–408, June 2010.

[18] C. Oshman, B. Shi, C. Li, R. Yang, Y. C. Lee, G. P. Peterson, et al., "The development of polymer-Based flat heat pipes," *J. Microelectromech. Syst.*, vol. 20, pp. 410–417, Apr. 2011.

[19] H. Chang, G. Wang, A. Yang, X. Tao, X. Liu, Y. Shen, et al., "A transparent, flexible, low-temperature, and solution-processible graphene composite electrode," *Adv. Funct. Mater.*, vol. 20, pp. 2893–2902, Sep. 2010.

[20] C. Feng, K. Liu, J. S. Wu, L. Liu, J. S. Cheng, Y. Zhang, et al., "Flexible, stretchable, transparent conducting films made from superaligned carbon nanotubes," *Adv. Funct. Mater.*, vol. 20, pp. 885–891, Mar. 2010.

[21] S. Lips, F. Lefèvre, J. Bonjour, "Combined effects of the filling ratio and the vapour space thickness on the performance of a flat plate heat pipe," *Int. J. Heat Mass Transf.*, vol. 53, pp. 694–702, Jan. 2010.

[22] A. A. El-Nasr, S. M. El-Haggag, "Effective thermal conductivity of heat pipes," *Heat Mass Transf.*, vol. 32, pp. 97–101, Nov. 1996.

[23] RC Dorf. *The engineering handbook*, 2nd ed., Boca Raton, CRC Press, 2004.

C. C. Chen was born in Taipei, Taiwan, October 13, 1984. The author received his master's degree in mechanical and mechatronic engineering from National Taiwan Ocean University, and now is a Ph.D candidate at the Department of Mechanical Engineering, National Taiwan University, Taipei. His major of study is energy, heat transfer, desiccant dehumidification and energy services.

He as a research assistant in the Prof. Sih-Li Chen's Energy lab for two years, for the period of time, he carried out many research project.

S. L. Chen was born in Nantou, Taiwan, September 14, 1956. The author received his Ph.D. degree in mechanical engineering from University of California at Berkeley and his M.S. degree in mechanical engineering from the National Taiwan University. His research is in the areas of phase change, heat transfer, HVAC, and energy engineering.

He is currently a Professor in the Department of Mechanical Engineering, the National Taiwan University, Taiwan, where he is leading the Energy Laboratory.

Prof. Chen has published more than 100 academic journal papers, 31 conference papers, and several patents. The article "Development of an intelligent energy management network for building automation" was accepted by the *IEEE Transactions on Automation Science and Engineering*, and the article "Numerical Simulation of Air Flow in the Mini-environment and SMIF Enclosure" was accepted by the *IEEE Transactions on Semiconductor Manufacturing*, and the paper was published on February 2003.